16th World Conference on Earthquake Engineering, 16WCEE 2017
Santiago Chile, January 9th to 13th 2017
Paper N° 450 (Abstract ID)
Registration Code: S-T1464737601

INUNDATION MODELING TO CREATE 2,500-YEAR RETURN PERIOD TSUNAMI DESIGN ZONE MAPS FOR THE ASCE 7-16 STANDARD

Y. Wei[(1)(2)], H.K. Thio[(3)], V. Titov[(4)], G. Chock[(5)], H. Zhou[(6)(7)], L. Tang[(8)], and C. Moore[(9)]

(1) Research scientist, University of Washington, Seattle, Washington, USA, yong.wei@noaa.gov
(2) Research Scientist, NOAA Center for Tsunami Research, Pacific Marine Environmental Laboratory, NOAA, Seattle, Washington, USA
(3) Principal Seismologist, AECOM Los Angeles, CA, USA, hong.kie.thio@aecom.com
(4) Research Scientist, NOAA Center for Tsunami Research, Pacific Marine Environmental Laboratory, NOAA, Seattle, Washington, USA, vasily.titov@noaa.gov
(5) President, Martin & Chock, Inc., Honolulu, Hawaii, USA, GChock@martinchock.com
(6) Research scientist, University of Washington, Seattle, Washington, USA, hongqiang.zhou@noaa.gov
(7) Research Scientist, NOAA Center for Tsunami Research, Pacific Marine Environmental Laboratory, NOAA, Seattle, Washington, USA
(8) Applied Research International, Seattle, Washington, USA, liujuan.tang@gmail.com
(9) Research Scientist, NOAA Center for Tsunami Research, Pacific Marine Environmental Laboratory, NOAA, Seattle, Washington, USA, christopher.moore@noaa.gov

Abstract

A national standard for engineering design for tsunami effects has not existed before and this significant risk is mostly ignored in engineering design. The American Society of Civil Engineers (ASCE) 7 Tsunami Loads and Effects Subcommittee has completed a chapter for the 2016 edition of ASCE/SEI 7 Standard. Chapter 6, Tsunami Loads and Effects, would become the first national tsunami design provisions. In this paper, we describe the methods, procedures, and results to create the 2,500-year tsunami design zone maps for Alaska, Washington, Oregon, California, and Hawaii. This ensures the probabilistic criteria are established in the tsunami design maps for their use with the ASCE 7-16 design provisions. These new tsunami design zone maps define the coastal zones where structures of greater importance would be designed for tsunami resistance and community resilience.

Keywords: Tsunami design zone, ASCE 7-16, probabilistic tsunami hazard assessment, tsunami loads and effects

1. Introduction

In the U.S., there has never been a national standard for engineering design for tsunami effects. The American Society of Civil Engineers (ASCE) 7 Tsunami Loads and Effects Subcommittee (TLESC) completed a comprehensive chapter fot the ASCE/SEI 7 Standard, *Minimum Design Loads and Associated Criteria for Buildings and Other Structures*, for proposed incorporation into the 2016 edition of the Standard. Chapter 6, *Tsunami Loads and Effects*, will become the first national tsunami design provisions established in a standard referenced in the International Building Code. States included in the scope of these provisions would be Alaska, Hawaii, California, Washington and Oregon. These provisions will require tsunami design of essential facilities and critical infrastructure in the tsunami design zone (TDZ).

The new ASCE standard recommends two procedures to obtain the inundation depth and velocities at a site of interest. The first procedure uses the Probabilistic Tsunami Hazard Analysis (PTHA) Offshore Tsunami Amplitude, wave period and other waveform parameters as input for a two-dimensional model to compute the tsunami inundation and flow velocities. The second procedure, named the Energy Grade Line (EGL) analysis, uses the PTHA runup elevation and associated inundation distance as input for a hydraulic analysis along topographic transects through the onshore structure. The runup elevation and inundation distance are indicated by the probabilistically based tsunami design zone maps provided through the work described in this paper.

In the next sections, we describe the methodology, procedure and results of the development of the ASCE 2,500-year Tsunami Design Zone (TDZ) maps based on the PTHA Offshore Tsunami Amplitude, i.e., the Maximum Considered Tsunami amplitudes at 100 m depth offshore.

2. Methods

2.1 PTHA offshore maximum tsunami amplitude

Probabilistic hazard maps are the key criteria necessary to establish risk-consistency for engineering design provisions. Probabilistic Tsunami Hazard Analysis (PTHA), adapted from the Probabilistic Seismic Hazard Assessment (PSHA), assesses tsunami risks based on a reliability analysis that considers the uncertainty and variability of seismic events. PTHA methods are widely used in United States [1, 2, 3], Japan [4], Australia [5, 6] and New Zealand [7]. Thio et al. [3] established a PTHA approach consisting of a large number of tsunami scenarios that included both epistemic uncertainties using logic trees as well as aleatory variability. Their study provides probabilistic offshore tsunami amplitudes along California's coastline. They also utilized the Offshore Tsunami Amplitudes as the reference of input for tsunami inundation for several coastal communities in California. For critical facilities and structures of greater importance, the PTHA method provides a probabilistic characterization of flow characteristics. The ASCE tsunami design criteria were developed with consideration of the hydrodynamic and geometric factors affecting the forces imparted to the structure and the variability in the capacity of the structural elements subjected to the flow. Thus, the design hazard is probabilistic and the corresponding design methodology is risk-based on structural performance and reliability.

Thio et al. [3] described the details of obtaining the 2,500-year offshore maximum tsunami amplitude. The methodology used by Thio et al. [3] is mostly adopted from the PSHA proposed by McGuire [8], except the PTHA is interested in the exceedance of maximum tsunami amplitude. Thio et al. [3] employed shallow water wave models to establish a database of Green's function for each of a set of subfaults that adequately describe the earthquake rupture. They then synthesize tsunami waveforms for any slip distribution by summing the individual subfault tsunami waveforms, and thus assemble the maximum Offshore Tsunami Amplitude of the wave along the 100 m water depth offshore. The methods in Thio et al. [3] include consideration of both aleatory and epistemic uncertainties, which account for uncertainties resulting from the random nature of modeling, as well as uncertainties due to incomplete understanding of natural processes of the earthquake sources. As the first step of developing the ASCE TDZ maps, this method [3] is used to obtain the ASCE PTHA offshore amplitudes for all five Pacific states of the U.S., including Alaska, California, Hawaii, Oregon and Washington[9]. This approach also provides source disaggregation, identifying the source regions and magnitudes that contribute the most to those Offshore Tsunami Amplitudes. Based on the PTHA source disaggregation, we reconstruct tsunami sources to the detail of source parameters so that the reconstructed tsunami scenarios provide good approximation of the PTHA offshore amplitudes at a site of interest. As a result, we are able to extend the PTHA offshore amplitudes to obtain the 2,500-year TDZ using tsunami inundation models. Fig. 1 shows an example of the PTHA maximum tsunami amplitude at 100 m depth offshore of Crescent City, California. In Fig.1, the color bars indicate the PTHA offshore maximum tsunami amplitude and the gray bars are the corresponding wave periods. The typical 2500-year maximum tsunami amplitude at 100 m water depth near Crescent City is about 25 ft (~ 7.6 m).

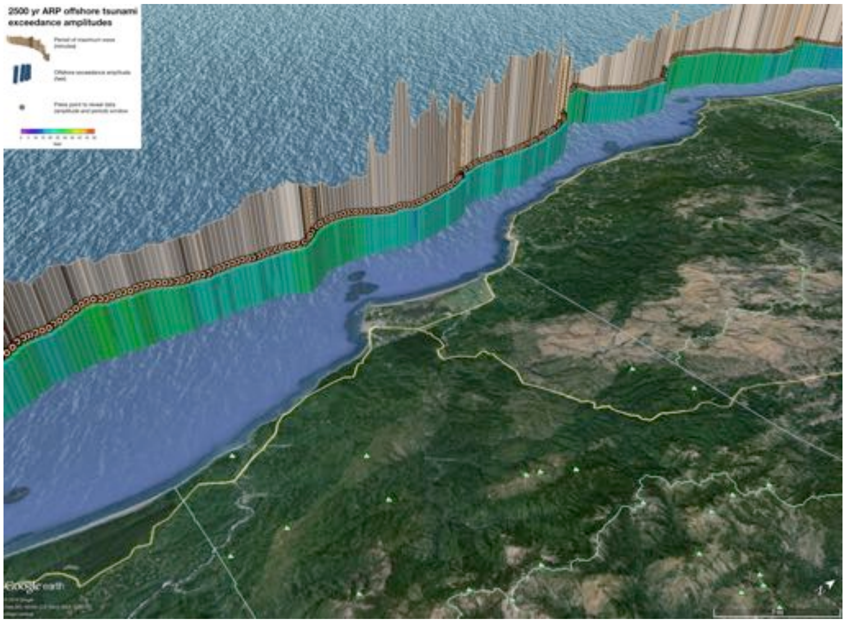

Fig. 1 – PTHA offshore maximum tsunami amplitude for Crescent City, California

2.2 Tsunami model

We use the Method of Splitting Tsunami (MOST) for tsunami propagation and inundation modeling. MOST is a suite of integrated numerical codes capable of simulating tsunami generation, transoceanic propagation and subsequent inundation of coastal areas [10]. The model employs a finite-difference approximation of the characteristic form of the shallow water wave equations by use of the splitting method [11]. For propagation, MOST uses the shallow water wave equations in spherical coordinates with numerical dispersion to account for different propagation wave speeds at different frequencies. MOST uses nested computational grids to telescope down to the high-resolution area of interest for inundation computation. The numerical coupling between all nested grids in MOST is unidirectional from the outer grid. MOST has been extensively tested against a number of laboratory experiments and benchmarks, and was successfully used for simulation of many historical tsunami events [12, 13, 14, 15, 16, 17, 18, 19].

2.3 Tsunami propagation database

Implementing MOST, the NOAA Center for Tsunami Research (NCTR) has developed a database of pre-computed unit tsunami propagation scenarios (Fig. 2). A unit tsunami propagation contains results of a model tsunami propagation scenario generated by a unit tsunami source with 1 m slip over an area of 100 km x 50 km. These unit sources are placed along all subduction zones and known tsunamigenic faults, and are aligned to fit known fault geometries (Fig. 2). Gica et al. [19] provides detailed descriptions of all unit sources with tabulated source parameters for each unit source, including their locations (longitude and latitude), focal depths, strikes and dips. The rake angles are all set to 90° for all unit sources. These parameters are used as model input for an elastic deformation model of Okada [20] to compute the vertical deformation resulting from a 1 m slip. This deformation is assumed to be instantaneously transferred to the ocean surface, and is considered a unit tsunami source. The tsunami propagation database consists of thousands of sets of pre-computed model results of tsunami propagation, generated by the unit tsunami sources computed at a grid resolution of 4 arc min (~ 7.2 km). Because of the linearity of tsunami waves in deep water, we can reconstruct a tsunami source (usually a combination of the unit scenarios) inverted from deep-water waveforms obtained from either observations or numerical solutions.

It is worth pointing out that the existing propagation database should not be directly used as solutions for water depth shallower than 1000 m due to the coarse resolution of the grids. However, all PTHA offshore amplitudes are available at the 100 m water depth. To solve this issue, we extended the existing database to include an additional database of tsunami waveforms computed using a grid resolution of 24 arc sec (~ 720 m). For coastlines of interest, we develop model grids of 24-arc-sec resolution to compute waveforms at the PTHA offshore points, adopting boundary conditions provided by the existing propagation database.

In the present study, we use the existing unit tsunami scenarios and the extended propagation database to reconstruct the disaggregated PTHA sources through an inversion method. This inversion process searches for a best match between the PTHA offshore wave amplitudes and the MOST-computed results, the details of which are provided in Section 2.4.

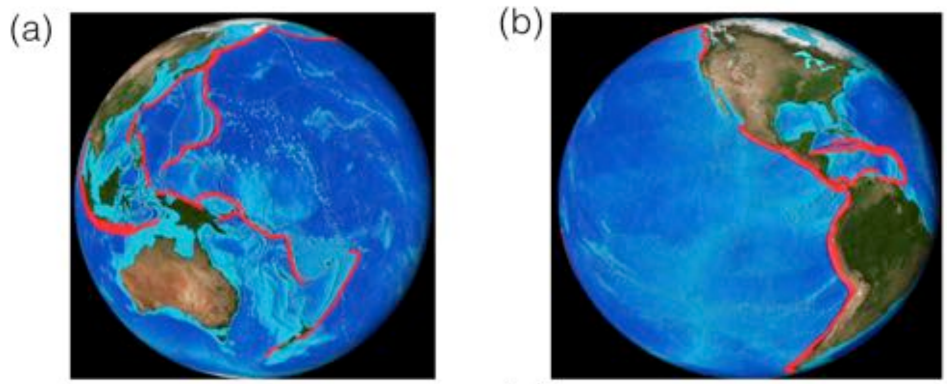

Fig. 2 – Tsunami unit sources as indicated by the red rectangles: (a) unit sources developed for western Pacific; (b) unit sources developed for eastern Pacific.

2.4 Tsunami propagation database

The PTHA approach of obtaining 2,500-year offshore maximum tsunami amplitude consists of tens of thousands of numerical results of synthetic scenarios [3]. A small subset of these synthetic scenarios is used to compute the inundation zone. For example, Thio et al. [3] applied only scenarios that were selected based on their source disaggregation study, and Power et al. [7] chose the largest 100 tsunamis for their probabilistic inundation study. Similarly, we choose only the source regions and magnitudes contributing the most to those offshore tsunami amplitudes at sites of interest. Figure 3 shows an example of the source disaggregation obtained [3]. For a site (122.0°W, 36.58°N) offshore of Monterey Bay, California, this source disaggregation map indicates that the most dominating source regions are the Aleutian Trench and the Alaska subduction zone. Therefore, for this site, we reconstruct tsunami sources from these two rupture areas, to produce model results matching the PTHA offshore amplitudes.

We use a nonlinear least squares method to realize the reconstruction of the tsunami sources. Based on the PTHA source disaggregation, we first select a group of unit sources in the dominating rupture zones. The inversion method then adjusts the combination of the slip amount of each unit source until the model results match the PTHA offshore amplitudes. The nonlinear least squares method, expressed in Eq. (1), starts with an initial guess of slips for selected unit sources. This provides an initial tsunami source. We can then quickly obtain the maximum tsunami amplitudes at every PTHA offshore point through a linear combination of the pre-computed propagation waveforms weighted by the slip amount. These model results are then compared with the PTHA values. The inversion method iteratively modifies the slip combination for those selected unit sources until a minimum least squares error is reached between the model results and the PTHA offshore amplitudes. We then further refine the slip combination until two conditions are satisfied: (1) the absolute error between the model results and the PTHA is less than 20%; and (2) all individual model results are greater than 80% of the

PTHA values. As a result, the final solution of slip combination for the selected unit sources gives us a workable tsunami source to compute the tsunami inundation.

$$\min_x \| f(x) \|_2^2 = \min_x \left(\sum_{j=1}^{n} f_j(x)^2 \right)$$

$$f_j(x) = \max\left[\sum_{i=1}^{m} \eta_{ij}(t) \cdot x_i \right] - A_j \tag{1}$$

where $\eta_{ij}(t)$ is the wave amplitude time series at point j due to i_{th} unit source; x_i is the slip coefficient on the i_{th} unit source; and A_j is PTHA offshore amplitude at j_{th} point.

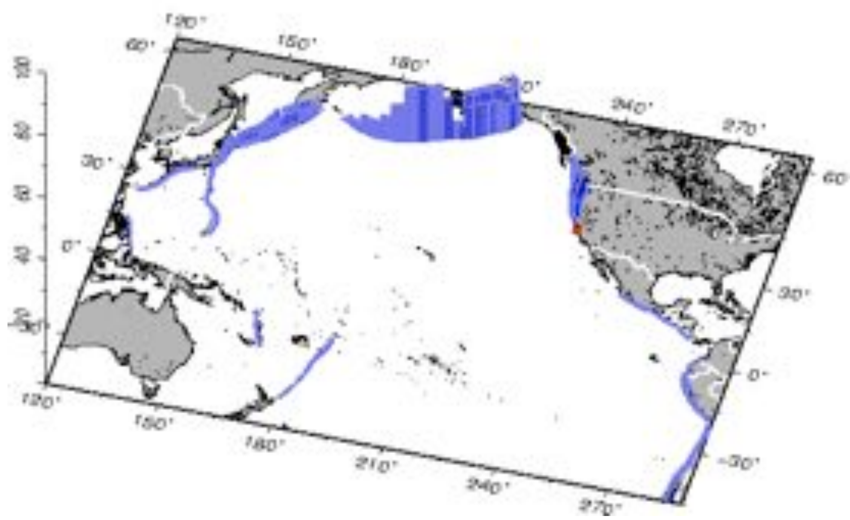

Fig. 3 – 2500-year PTHA source disaggregation for a site (122.0°W, 36.58°N) offshore of Monterey Bay, California, where the blue bars denote the source contributions (%) to the site indicated by the red circle.

2.5 Digital Elevation Models (DEM)

The National Geophysical Data Center (NGDC) has been building high-resolution digital elevation models (DEMs), mostly at a grid resolution of 1/3 arc sec (~ 10 m) of bathymetry and topography for selected U.S. coastal regions [21]. The DEMs are part of the U.S. tsunami forecast system developed for NOAA's Tsunami Warning Centers. These DEMs have 1) a global, geographic coordinate system; 2) a mean high water (MHW) vertical datum for modeling of maximum flooding; 3) a grid file format of the ESRI Arc GIS; and 4) bare earth with buildings and trees excluded from the DEM. Most coastal regions along the U.S. West Coast are covered by these high-resolution DEMs. In Hawaii, 1/3-arc-sec DEMs are developed for most of the islands. The exceptions are east of Maui, which has a coarser grid resolution at 1 arc sec (~ 30 m), and western and central Molokai and the southern tip of the Island of Hawaii have a grid resolution of 6 arc sec (~ 180 m). In Alaska, high-resolution DEMs are only available for populated areas, and nearly 90% of these "high-resolution" DEMs only have a grid resolution of 1 arc sec (~ 30 m) or lower.

2.6 Setup of the tsunami inundation models

After the tsunami sources for coastal regions of interest are determined by the method described above, MOST is used to compute the ASCE TDZ. It is not realistic to carry out all inundation computations at a grid resolution of 1/3 arc sec (~ 10 m) for all coastlines due to the large coverage area of the coastlines and available time for completing the ASCE TDZ. Instead, we use an optimal grid resolution of 2 arc sec (~ 60 m) for inundation computation in MOST. A typical grid resolution of 2 arc sec (~ 60 m) is used for forecast models developed for NOAA's Tsunami Warning Centers to forecast inundation along U.S. coastlines. In many cases, the inundation areas obtained using 2 arc sec (~ 60 m) are similar to those using a grid resolution of 1/3 arc sec (~ 10 m) [13]. The bathymetry and topography of all model grids are derived from NGDC's DEMs based on their best-available data at the site. The vertical datum for all inundation computation is the MHW. A constant Manning's coefficient of 0.03 is applied to all inundation computation.

As discussed in Section 2.2, MOST uses telescoped grids (A, B and C grids) to account for tsunami wave transformation from deep water to onshore flooding. For a coastline of interest, we use the 24-arc-sec grid described in Section 2.3 as the A grid of MOST. A smaller B grid, with a grid resolution of 6 arc sec (~ 180 m), is nested within the A grid to further capture tsunami wave characteristics at water depths of hundreds of meters. The 2-arc-sec (~ 60 m) grid is used at the innermost level, the C grid, to compute tsunami inundation. Figure 4 illustrates all C grids used to develop the ASCE TDZ for the U.S. West Coast. In the present study, we use a total number of 19 models to provide full coverage for the coastal regions of U.S. West Coast. The bathymetry and topography of all model grids, including the A, B and C grids, are derived from NGDC's DEMs based on their best-available data at the site, so the vertical datum for all inundation computation is the MHW. A constant Manning's coefficient of 0.03 is applied to all inundation computation.

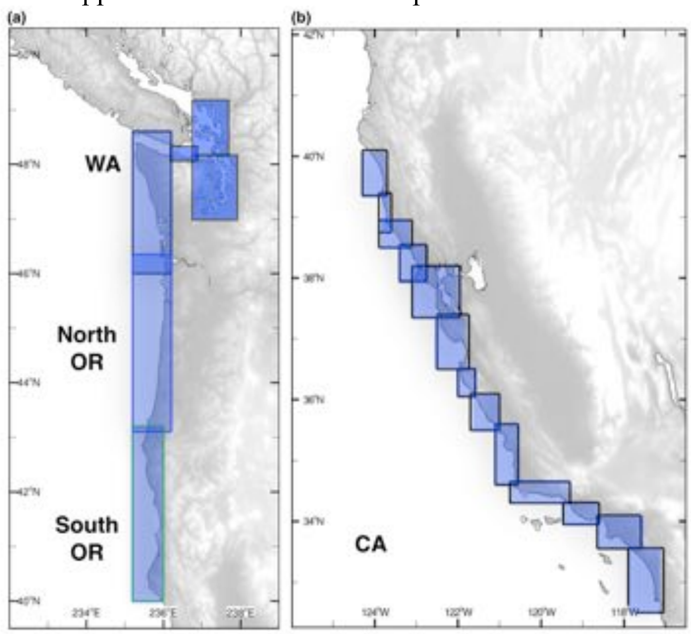

Fig. 4 – Model coverage of all C grids for MOST inundation computation along the U.S. West Coast. (a) Washington and Oregon; (b) California.

3. Results and discussion

3.1 Reconstructed tsunami sources

The PTHA analysis indicates that the 2500-year tsunami hazards along the coastal regions of Washington, Oregon and northern California are dominated by tsunamis generated in the Cascadia Subduction Zone (CSZ). The PTHA maximum tsunami amplitudes at 100 m water depth offshore are in the range of 4 to 12 m (blue circles in Fig. 5a). For near-field sources, we assume the maximum tsunami amplitudes offshore are mostly dominated by earthquake ruptures near the site of interest, e.g., within a couple of hundred kilometers. The impact caused by ruptures at farther distances than that is considered to be secondary. As a result, we break down the coastlines of Washington, Oregon and northern California into eight segments. We then use the inversion procedure described in Section 2.4 to obtain the valid source(s) for each of these segments. Figure 5 shows that these reconstructed tsunami sources give reasonable comparison between the model results and the PTHA values along the coastlines of the CSZ.

Table 1 summarizes some characteristics of the reconstructed source for each segment of coastlines. One can see that the range of average slip is between 19.3 m and 39.8 m, with the largest slip of 66.3 m and the smallest slip of 5.0 m. The equivalent earthquake magnitudes of these sources are between 8.79 and 9.09.

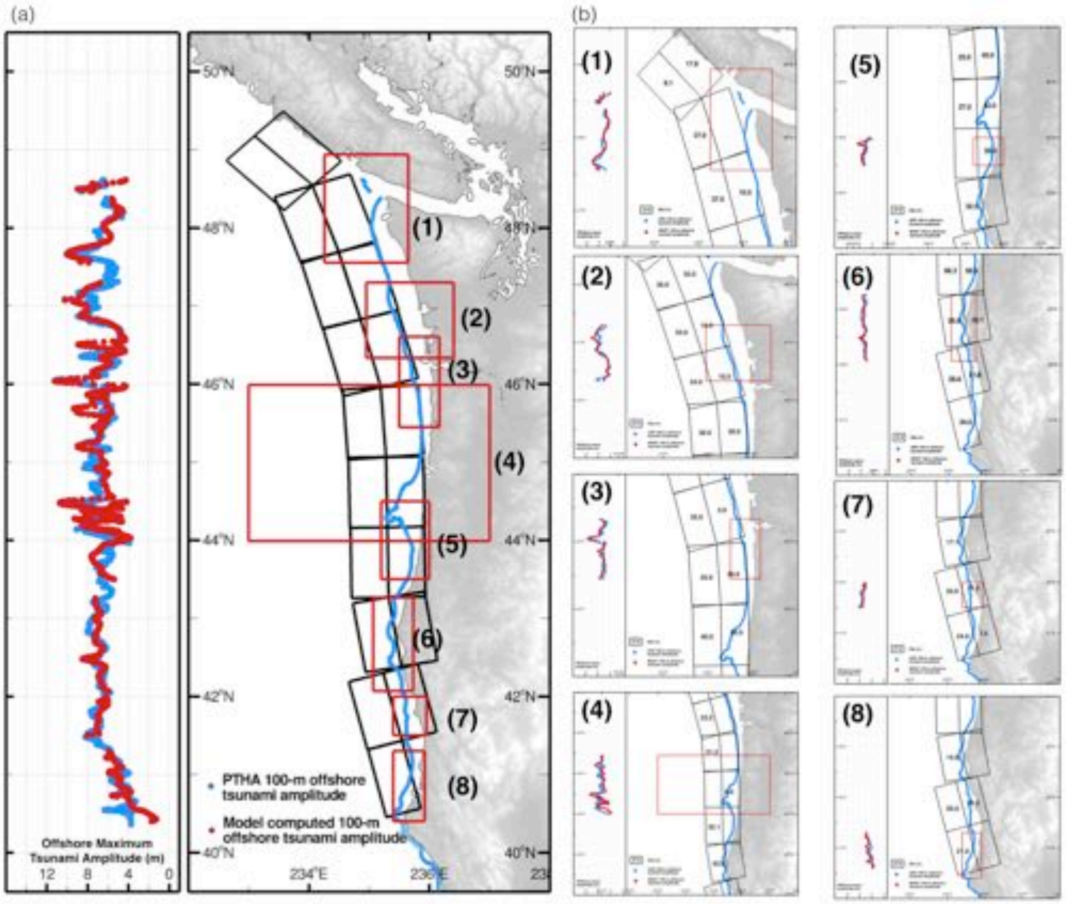

Fig. 5 – Reconstruction of the tsunami sources for coastlines dominated by the Cascadia Subduction Zone (CSZ), where the black boxes are the unit tsunami sources with dimensions of 100 km in length and 50 km in width, and red boxes are the 24-arc-sec grids to compute the maximum tsunami amplitudes for comparison with the PTHA values. (a) The left panel shows the comparison between model results (red circles) and the PTHA values (blue circles); the right panel shows the tsunami unit sources along the coastline of the CSZ, and the red boxes indicate the model coverage of the 24-arc-sec grids. (b) The breakdown of individual sources used to match the model results with the PHTA tsunami amplitudes. The value shown on the unit source is the slip associated with that unit source.

Table 1 – Characteristics of the reconstructed tsunami sources in the CSZ

Segment of coastlines	Average slip (m)	Largest Slip (m)	Smallest Slip (m)	Length of Source (km)	Equiv. EQ Magnitude
1	20.3	37.0	9.1	300	8.80
2	25.9	35.0	10.0	400	9.01
3	29.2	50.0	5.0	300	8.96
4	25.5	43.0	8.0	500	8.87
5	34.4	45.0	25.0	400	9.01
6	39.8	66.3	26.8	400	9.09
7	19.3	33.0	7.5	300	8.79
8	26.7	50.0	15.6	300	8.88

3.2 TDZ Maps Developed for ASCE7

Once the tsunami sources are determined, the tsunami models described in Section 2.6 are used to compute the TDZ, defined as the inundated areas between the shoreline and the inundation limit. We note here that the computational results obtained from a tsunami source are only valid for the segment of coastline used to reconstruct that source. When a segment of coastline is dominated by multiple tsunami sources, an envelope of the inundation areas is then used to define the final TDZ.

Figure 6 shows the TDZ for Westport, Washington, and Monterey, California. Figure 7 shows examples of the TDZ maps for Puget Sound, Washington. Inundation hazards from both distant and local sources are considered in Puget Sound TDZs. The distant tsunami impact comes from the 2500-year tsunami scenario in the CSZ, the tsunami source (1) shown in Fig. 5. The local impact comes from three potential local faults, the Seattle Fault, the Tacoma Fault, and the Rosedale Fault. The TDZ shown in Fig. 7 is the envelope of inundation hazards produced by all four scenarios.

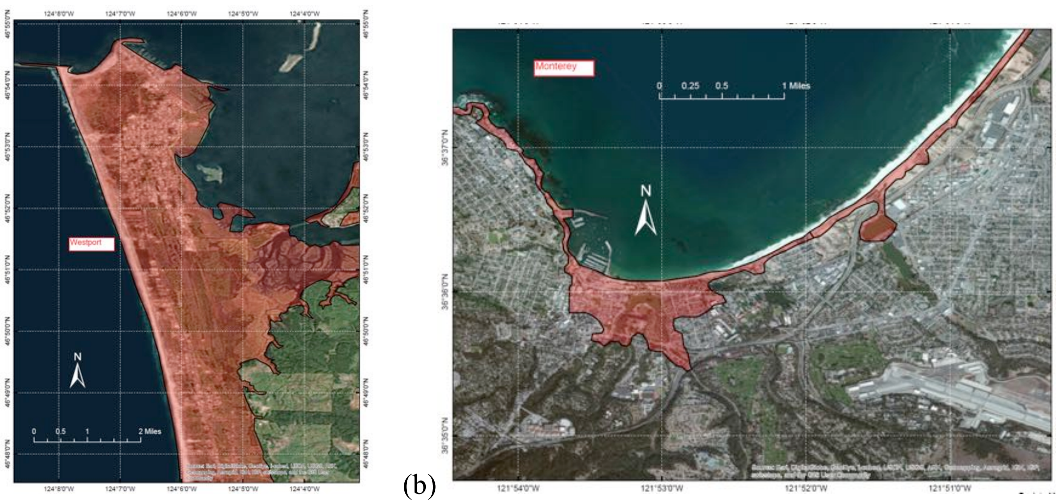

(a) (b)

Fig. 6 – (a) TDZ for Westport, Washington; (b) TDZ for Monterey, California.

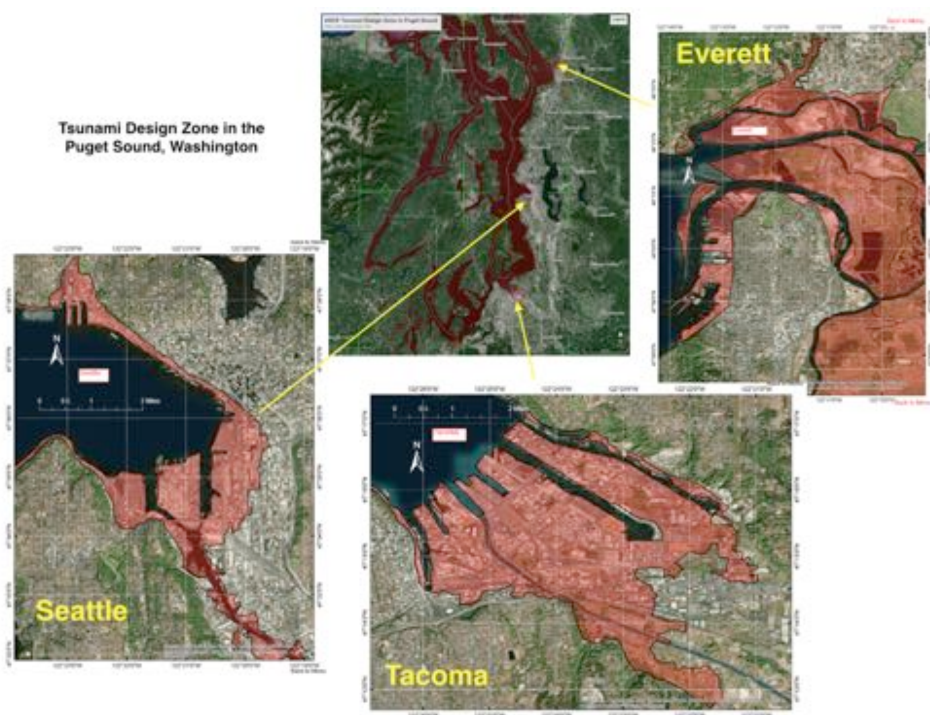

Fig. 7 – TDZ for Puget Sound, Washington.

4. Conclusions

The ASCE TLESC has completed a chapter of *Tsunami Loads and Effects* for the 2016 edition of ASCE/SEI 7 Standard to establish a national standard of engineering design for tsunami loads and effects. As a critical part of the ASCE 7 Standard, this study develops TDZ maps based on the 2500-year PTHA Offshore Tsunami Amplitudes at 100 m water depth offshore. The TDZ maps provide fundamental input of inundation distance and runup elevations for ASCE's Energy Grade Line (EGL) analysis for engineers to calculate the tsunami effects on specific structures in the TDZ. The TDZ maps are developed for a the entire coastlines of Washington, Oregon, California and Hawaii, and most of the Southern coastline of Alaska and the Aleutian Islands. We used an inversion process to reconstruct tsunami sources to match the model results with PTHA 2500-year maximum tsunami amplitudes offshore. These tsunami sources are then employed in inundation models to compute the TDZ at a grid resolution of 2 arc sec (~ 60 m).

The format of the TDZ products will include metadata, GIS layers, as well as paper example maps. Future efforts of improving these TDZ include higher-resolution inundation modeling using a grid resolution of 1/3 arc sec (~10 m) or finer for selected sites in coordination with the states and the National Tsunami Hazards Mitigation Program.

5. Acknowledgements

The authors are grateful to ASCE for funding this work. We are also grateful for the efforts and support of the ASCE 7 Tsunami Loads and Effects Subcommittee. This publication is partially funded by the Joint Institute for the Study of the Atmosphere and Ocean (JISAO) under NOAA Cooperative Agreement NA10OAR4320148 (2010-2015) and NA15OAR4320063 (2015-2020), JISAO Contribution No. 2713, PMEL Contribution No. 4503.

6. References

[1] GEIST E.L., PARSONS T (2006): Probabilistic analysis of tsunami hazards, Natural Hazards, 37, 272-314.

[2] GONZÁLEZ, F.I., GEIST, E.L., JAFFE, B., KANOGLU, U., MOFJELD, H., SYNOLAKIS, C.E., TITOV, V.V., ARCAS, D., BELLOMO, D., AND CARLTON, D. (2009): Probabilistic tsunami hazard assessment at Seaside, Oregon, for near- and far-field seismic sources, J. Geophys. Res., 114, C11023, doi:10.1029/2008JC005132.

[3] THIO H.K., SOMERVILLE P., POLET J. (2010): Probabilistic tsunami hazard in California, PEER report 2010.108, Pacific Earthquake Engineering Research Center, College of Engineering, University of California, Berkeley.

[4] ANNAKA, T., SATAKE, K., SAKAKIYAMA, T., YANAGISAWA, K., AND SHUTO, N. (2007): Logic-tree approach for probabilistic tsunami hazard analysis and its applications to the Japanese Coasts, Pure and Applied Geophysics, 164, 2007, 577-592.

[5] BURBRIDGE D., CUMMINGS P.R., MLECZKO R., THIO H.K. (2008): A probabilistic tsunami hazard assessment for western Australia, Pure and Applied Geophysics, 165, 2059-2088.

[6] CARDNO C.A. (2012): NSW tsunami inundation modeling and risk assessment, LJ2874/Rep2703, prepared for NSW Office of Environmental and Heritage and NSW State Emergency Service, 56 pp.

[7] POWER W., WANG X., LANE E., and GILLBREAND P. (2012): A probabilistic tsunami hazard study of the Auckland region, Part I: propagation modeling and tsunami hazard assessment at the shoreline, Pure and Applied Geophysics, 170, 1621-1634.

[8] MCGUIRE R.K. (2004): Seismic hazard and risk analysis, Earthquake Engineering Research Institute, Oakland, CA, 240 pp.

[9] THIO, H.K., WEI, Y., LI, W., AND CHOCK, G., (2017): Development of Offshore Probabilistic Tsunami Exceedance Amplitudes for ASCE 7-16, 16th World Conference on Earthquake Engineering, 16WCEE 2017, Santiago, Chile.

[10] TITOV V.V., GONZÁLEZ F.I. (1997): Implementation and testing of the Method of Splitting Tsunami (MOST) model, NOAA Tech. Memo. ERL PMEL-112 (PB98-122773), NOAA/Pacific Marine Environmental Laboratory, Seattle, WA, 11 pp.

[11] TITOV V.V., SYNOLAKIS C.E. (1997): Extreme inundation flows during the Hokkaido-Nansei-Oki tsunami. Geophys. Res. Lett., 24(11), 1315–1318.

[12] ZHOU H., WEI Y., TITOV V.V. (2012): Dispersive modeling of the 2009 Samoa tsunami. Geophys. Res. Lett., 39(16), L16603, doi:1029/2012GL053068

[13] SYNOLAKIS, C.E., BERNARD, E.N., TITOV, V.V., KANOGLU, U., AND GONZÁLEZ, F.I. (2008): Validation and verification of tsunami numerical models. Pure Appl. Geophys., 165(11–12), 2197–2228.

[14] TANG L., TITOV V.V., CHAMBERLIN C.D. (2009): Development, testing, and applications of site-specific tsunami inundation models for real-time forecasting, J. Geophys. Res., 114, C12025, doi:10.1029/2009JC005476.

[15] TANG L., et al. (2012): Direct energy estimation of the 2011 Japan tsunami using deep-ocean pressure measurements. J. Geophys. Res., 117, C08008, doi:10.1029/2011JC007635.

[16] TITOV V.V. (2009): Tsunami forecasting. Chapter 12 in The Sea, Volume 15: Tsunamis, Harvard University Press, Cambridge, MA and London, England, 371–400.

[17] WEI, Y., BERNARD, E.N., TANG, L., WEISS, R., TITOV, V.V., MOORE, C., SPILLANE, M., HOPKINS, M., AND KÂNOĞLU, U. (2008): Real-time experimental forecast of the Peruvian tsunami of August 2007 for U.S. coastlines. Geophys. Res. Lett., 35, L04609, doi:10.1029/2007GL032250.

[18] WEI Y., CHAMBERLIN, C., TITOV, V., TANG, L. AND BERNARD, E. (2013): Modeling of the 2011 Japan tsunami - Lessons for near-field forecast. Pure Appl. Geophys., 170(6–8), doi: 10.1007/s00024-012-0519-z, 1309–1331

[19] GICA E., SPILLANE M., TITOV V.V., CHAMBERLIN C., NEWMAN J.C. (2008): Development of the forecast propagation database for NOAA's Short-term Inundation Forecast for Tsunamis (SIFT). NOAA Tech. Memo. OAR PMEL-139, 89 pp.

[20] OKADA Y. (1985): Surface deformation due to shear and tensile faults in a half space, Bull. Seismol. Soc. Am., 75(4), 1135–1154.

[21] EAKINS B.W., TAYLOR L.A., Seamlessly integrating bathymetric and topographic data to support tsunami modeling and forecasting efforts, in Ocean Globe, ed. by J. Breman, ESRI Press, Redlands, 2010, pp. 37-56.